

MAPPING DEFORESTATION IN PERMANENT FOREST RESERVE OF PENINSULAR MALAYSIA WITH MULTI-TEMPORAL SAR IMAGERY AND U-NET BASED SEMANTIC SEGMENTATION

Muhammad Azzam A. Wahab¹, Ely Salwana Mat Surin^{2*}, Norshita Mat Nayan³ and Hameedur Rahman⁴

^{1,2,3}Institute of IR 4.0 (IIR4.0), Universiti Kebangsaan Malaysia, UKM Bangi, 43650 Selangor, Malaysia

⁴Department of Computer Science, HITEC University, Taxila, 47080 Punjab, Pakistan

Email: p100378@siswa.ukm.edu.my¹, elysalwana@ukm.edu.my^{2*} (corresponding author), norshitaivi@ukm.edu.my³, rhameedur@gmail.com⁴

DOI: <https://doi.org/10.22452/mjcs.sp2021no2.2>

ABSTRACT

Deforestation is the long-term or permanent conversion of forest land to other uses, such as agriculture, mining, and urban development. As a result, deforestation has catastrophic consequences for the environment, including the loss of biodiversity, disruption of clean water supplies, and the acceleration of climate change. According to statistics, the deforestation trend in developing countries is at an alarming rate including Malaysia where plantation activities are the primary cause of forest loss. Recent anecdotal studies have demonstrated the effectiveness of the deep learning-based (DL) approach in producing deforestation maps. However, there are limited studies concentrating on DL approach for synthetic aperture radar (SAR) imaging due to complexity of the computational concepts of the method. The SAR imagery can be challenging to interpret but its all-weather and all-day capability can be critical in forest monitoring compared to optical imagery. Thus, in this study, we propose to map deforestation areas in Permanent Forest Reserve (HSK) using multi-temporal Sentinel-1 SAR data. Deep learning-based U-Net was employed to classify the SAR imagery as forest and non-forest due to its semantic segmentation capabilities. The experiment results showed that the proposed deep learning-based technique successfully achieved 0.993 of intersection over union (IoU) and 0.980 of overall accuracy (OA). Also, we explained the entire procedure from beginning to end as simple as possible for beginners to comprehend. In brief, the findings of this study have the potential to improve monitoring of damaged HSK areas, prioritize the restoration of the affected forest areas and protecting the forest lands from illegal deforestation activities.

Keywords: *Deforestation, U-Net, Sentinel-1, OTBTF, Peninsular Malaysia*

1.0 INTRODUCTION

The impact of human activities makes the forest ecosystems even more prone to damage. Al Gore, an environmental activist and Nobel Peace Prize 2007 winner [1], once said that "Global warming, along with the cutting and burning of forests and other critical habitats, is causing the loss of living species at a level comparable to the extinction event that wiped out the dinosaurs 65 million years ago. That event was believed to have been caused by a giant asteroid. This time it is not an asteroid colliding with the Earth and wreaking havoc: **it is us**" [2]. In 2018, human activities has caused the destruction of 12 million hectares (30 million acres) of tropical tree cover in 2018 which equivalent to 30 football fields per minute [3]. Furthermore, a recent satellite-based study performed by Global Forest Watch found that the Earth's tree cover decreased by almost 260,000 square kilometres in 2020 [4]. The loss of rainforests may have a serious implication on global warming as these vegetation serves as "carbon sinks" to absorb carbon. Despite many attempts to prevent deforestation (i.e., REDD+¹), the efforts have deteriorated over the last 10 years, and Malaysia was one of the top fifteen nations in 2020 with significant losses [4], [5].

Malaysia is a complex natural phenomenon of tropical rainforests that are rich in forest resources covering 59.5 percent of the country's total land area [6]. However, Malaysia has suffered from forest loss as a result of land clearance for palm oil expansion as part of the country's economic contribution since the 1990s [7]. From 2014 to 2018, the palm oil sector contributed 5% to 7% of the country's Gross Domestic Product (GDP) on average, with export revenue averaging RM 64.24 billion per year [8]. Malaysia's growing palm oil production has raised concerns among western nations about deforestation and the country's failure to adhere to the best agricultural standards [9], prompting calls

¹ REDD+ is a United Nations international programme whose name is an abbreviation for 'reducing emissions from deforestation and forest degradation, conservation of existing forest carbon stocks, sustainable forest management and enhancement of forest carbon stocks'.

for a boycott of Malaysian palm oil, both refined and crude. Their report also revealed that the underlying cause of deforestation includes ineffective and flawed forest governance. For example, a study by [10] indicated that the most significant problem limiting forest law enforcement authorities' ability to perform surveillance on logging activities regions was 'enforcement factors' (i.e., insufficient workforce and restricted funds). The authors also noted a lack of intelligence-based information among forest law enforcement authorities, as well as lack of modern technology to monitor the vast area of forest. Thus, it is the government's responsibility to address the vulnerabilities inherent in the present system and create appropriate solutions for managing forests, fighting desertification, halt and reverse land degradation. However, prior research has mostly concentrated on factors such as mining, large-scale commercial oil palm plantations, agriculture, road development, and dams. Minimal attention is devoted on sought-after technologies like remote sensing (RS), unmanned aerial vehicle (UAV), and light detection and ranging (LiDAR) for forest monitoring tasks [11]. Therefore, this paper aims to bridge the gap by examining the advantages of RS technology, which is one of the most efficient and cost-effective ways compared to other technologies to stop wasteful deforestation activities on a large scale.

1.1 Forest Monitoring In Malaysia

RS satellites are a very effective tool for ecological monitoring, particularly over vast areas. Given the dynamics of large-scale RS observation, RS sensors are capable of sensing more spectral bands than human eyes, enabling the modelling and retrieval of diverse ecological indicators (i.e., vegetation indices). On the other hand, ground-based monitoring which commonly employed for environmental monitoring, is region-limited, time-consuming, expensive, labour-intensive and only suitable for point-based environmental monitoring in a small area [12]. As such, the use of RS images has become critical for monitoring forest changes over time where the Forestry Department of Peninsular Malaysia (JPSM) has done an excellent job of integrating them [13].

There are two basic types of RS imaging data distinguished by their energy source: passive and active system [14]. A passive system (i.e., Sentinel-2, Landsat 8, PlanetScope, SPOT²-6, SPOT-7, Worldview) uses the sun as a source of reflected electromagnetic radiation. It then measures the electromagnetic radiation aboard the RS platform – the data sometimes referred to as optical imagery. An active system (i.e., Sentinel-1, ENVISAT³, ERS⁴, ALOS PALSAR⁵, TerraSAR-X, RADARSAT⁶-2) use its own energy and then measures the amount of that electromagnetic radiation reflected back after interacting with the Earth's surfaces – the data sometimes referred to as Synthetic Aperture Radar (SAR) imaging. In Malaysia, the Malaysian Space Agency (MYSA) is responsible for directing the country's research and development (R&D) activities in RS, as well as managing RS data in a strategic, organized, and comprehensive manner [15].

In accordance with the National Blue Ocean Strategy (NBOS) initiative, JPSM, in collaboration with the State Forestry Department and the MYSA, launched the Forest Monitoring Using Remote Sensing (FMRS) system in 2014 with the objective of providing a platform of optical imagery for forest rangers to monitor and enforce in permanent and non-permanent forest reserves throughout Peninsular Malaysia [16]. The system has proven to effectively decrease timber smuggling nevertheless, the system relies on conventional optical satellite imaging, which suffers from cloud obstructing the area of interest. [17], [18]. In any of their operations, JPSM has not yet implemented SAR imaging data [19] due to complexity of processing, interpreting, and analysing SAR data which consistent with the issues reported in [20]. Nevertheless, SAR imagery is regarded as one of the best options to obtain high-resolution images regardless of daylight or weather conditions. This will benefiting tropical countries in developing early warning systems for efficient assessment and monitoring of forest resources [21]. Furthermore, when combined with polarimetric, interferometric, and topographic data, SAR imaging is ideal for forest mapping applications [21]–[24]. Numerous studies have investigated SAR-based change detection approaches to overcome the limitation of cloud-free optical imagery; for example, pixel-based ratio methods [25], algebra-based methods [26], and transformation-based methods [27], but they all rely on inefficient data for monitoring change [21]. Traditional model-driven techniques are becoming inadequate to satisfy the requirements of big data applications as data scales increase. To comprehend and evaluate forest resources, modern and up-to-date technique is needed. This discovery paved the way for clever processing techniques based on deep learning. These techniques are particularly effective in natural image processing and remote sensing [28].

² SPOT is an abbreviation for *Satellite pour l'Observation de la Terre*, a commercial Earth satellite from France.

³ ENVISAT is an abbreviation for *Environmental Satellite*, operated by the European Space Agency.

⁴ ERS is an abbreviation for *European Remote Sensing* satellite, operated by the European Space Agency.

⁵ ALOS PALSAR is an abbreviation for *Advanced Land Observing Satellite Phased Array Type L-band Synthetic Aperture Radar*, operated by Japan Aerospace Exploration Agency.

⁶ RADARSAT is an abbreviation for *Radar Satellite*, operated by the Canadian Space Agency.

The rapid advancements in pattern recognition and artificial intelligence have led to the development of new geospatial data mining tools, allowing precise monitoring of forest ecosystems [29], [30]. Furthermore, this approach opens new opportunities and perspectives for applying DL methods to various environmental science research and development issues. Malaysia, on the other hand, falls behind other nations in terms of using DL for forest monitoring studies [31]. Indonesians, for example, have created a deep learning model called ForestNet that utilizes satellite images to automatically detect the causes of forest loss. ForestNet is said to outperform other standard classification methods [32] the procedures and processes were complex to understand. The authors in [33] agrees with our point of view that many beginners find it challenging to follow current literature due to the complexity of the stages and a large number of calculations. Therefore, it encourages us to invest time and effort into this study by providing an easy-to-follow strategy that enables scholars to get started quickly. Secondly, the model in [32] is unsuitable for SAR imagery data because it was developed using optical imagery data from the Landsat-8 satellite. In other words, RGB (Red, Green, Blue) representations are preferred over black and white of SAR data. Acknowledging these limitations, our research will include a discussion of deep learning approaches in the context of SAR imagery data used for forest monitoring.

The purpose of this research is to assess the feasibility of deforestation mapping using dual-polarization SAR imaging data of HSK Yong, Pahang and compare between deep learning and conventional machine learning performances. The main contribution is two folds:

- i. Will get a better understanding to develop deep learning and classical machine learning classification schemes for deforestation mapping.
- ii. Will get a better understanding of the SAR imagery data usage in forest management.

2.0 BACKGROUND AND RELATED WORKS

This study is an extension of work that has initially been accepted and presented at the 5th International Conference on Information Retrieval and Knowledge Management 2021 (CAMP'21), which was organized by the *Persatuan Capaian Maklumat dan Pengurusan Pengetahuan* (PECAMP) [31]. The original work is titled "An Approach to Mapping Deforestation in Permanent Forest Reserve Using the Convolutional Neural Network and Sentinel-1 Synthetic Aperture Radar" [34]. The extension focuses on a new approach based on semantic segmentation as an alternative to the previously employed patch-based classification of convolutional neural network (CNN) while retaining the original reviews, gaps and the study area. In particular, we developed a U-Net-like architecture for mapping deforestation in Peninsular Malaysia's Permanent Forest Reserve (HSK). Additionally, the data sets were expanded to include temporal data collections that included ascending and descending polarimetric channels as depicted in Fig. 9.

Another critical point to examine that was left out in [34] is how DL semantic segmentation outperforms the classical machine learning (ML) method (i.e., random forest, support vector machine, etc.). Numerous relevant issues may be addressed using classical ML methods as their accuracy are comparable to DL methodologies [35]. For example, recent studies [36], [37] indicate that random forest (RF) achieves excellent accuracy even with small sample sizes making it well-suited for complex and simple classification tasks. In [38], the performance of maximum likelihood, support vector machine (SVM), and RF are compared for the classification of land cover and forest types using SAR imagery. The overall accuracy of RF algorithm consistently outperformed the others in the respective classification tasks. The RF classifier also outperformed SVM classifier in the classification of Mediterranean forest area [39]. Additionally, the SVM classifier failed to perform due to unbalanced classes in the sample sets. Given the above, RF classifier could be well suited as a baseline model for comparison [40].

Previously in [34], CNN's patch-based classification achieved an OA of 81.57 percent but the outputs still experienced unbalanced classification due to the coarse resolution of Sentinel-1 data and speckle noise effects. Increasing the resolution of SAR data will require a new orbit planning, platform, payload, and signal processing system, all which are prerequisites for improving the performance of SAR applications [41]. That is not possible in our case since we are utilising publicly available data. For speckle noise effects issue, various speckle reduction techniques are available in literature such as the Mean Filter, Median Filter, Lee-Sigma Filter, Lee Filter, Gamma-MAP Filter, and Frost Filter. When selecting a speckle reduction method, it is important to evaluate which technique provides the most textural information [42], [34], [43]. Thus, we believe that U-Net's semantic segmentation-based classification will outperform CNN's patch-based classification since semantic segmentation approaches use the semantic spatial context to train networks to estimate the semantic of patches of pixels rather than a single pixel [44]. Additionally, semantic

segmentation has the benefit of improving accuracy by eliminating unwanted background noise which was not addressed in the previous research. [45]. In light of this, we decided to employ the aforementioned method and discussed relevant studies in the following sub-sections to assist demonstrate the importance of this suggested method.

2.1 Semantic Segmentation Using SAR Images

The semantic segmentation generates a fine-grained delineation of objects that incorporates their spatial information [46]. For semantic segmentation of RS images, spatial precision at the pixel-level is critical for classification, particularly at the borders of various objects [47]. Environmental monitoring, crop cover and type analysis, forest species classification, building categorization, and land use analysis in urban areas are all proven examples of semantic segmentation with remote sensing imagery [46]. There are three important aspects outlined in [46] for adapting deep learning methods to the segmentation of remote sensing imagery. First, pixel-level precision must be maintained. Second, using a high number of channels such as Hyperspectral Images (HSI) is not recommended. Finally, a sufficient number of training examples is required for a high-quality model. These aspects will provide a strong basis for our research, especially in the section on experimental design [46].

The advantage of SAR image segmentation over optical segmentation is the convenience of performing texture analysis (i.e., transform domain, statistical, etc.) [48]. A typical texture analysis technique for extracting spatial characteristics from a SAR image is using the RGB bands of a false-color composite image. The RGB bands of the false-color composite image are then used to train deep learning models to perform semantic segmentation [48]. For example, [49] formed a false colored RGB image from C-band Radarsat-2 data to distinguish between various land use and land cover (LULC) classes. This technique has the potential to enhance visualizations to the level of optical imaging.

Given the volume of data collected regularly by various satellite sensors, RS researchers have made significant efforts to incorporate LULC classification using DL and SAR. For example, the work by [50] experimented with six DL architectures for land cover mapping and classification: Pyramid Scene Parsing, U-Net, DeepLabv3+, Path Aggregation Network, Encoder-Decoder Network and Feature Pyramid Network. Although much of their work focused on various land cover classes (urban, forest, water, and agriculture) rather than specifically on deforestation, their contribution to the present work is significant: first, multi-temporal (time-series) SAR datasets offer a unique opportunity to provide reliable information and speckle reduction inhomogeneous regions systematically. Thus, ensuring semantic segmentation approaches can effectively detect spatial patterns during the training phase and make models more robust for feature extraction [50]. Secondly, standard accuracy metrics, such as evaluation metrics, do not work well in areas with a high disparity in land cover classes. Thus, the Jaccard Index coefficient, also known as intersection over union (IoU), can be used [50]. Lastly, [50] ranked all six deep learning as follows (IoU closer to 1 the better): Pyramid Scene Parsing (0.64431), U-Net (0.61819), Encoder-Decoder Network (0.61381), DeepLabv3+ (0.61245), Path Aggregation Network (0.59816), and Feature Pyramid Network (0.57484).

Equally important, an on-demand Google Earth Engine (GEE) provides massive RS images and pre-processed data suitable for machine learning and deep learning. For example, [51] proposed a fully automatic processing chain for detecting disturbances in tropical seasonal forests using Sentinel-1 data and Landsat-8. Although they demonstrated that Sentinel-1 had a lower overall accuracy (OA) than Landsat-8, the authors agreed that both have significantly reduced the average time lag for detecting disturbances, contributing to more actionable information for decision-making. Likewise, a recent study by [52] has introduced an Early Warning System (EWS) for near real-time detection of deforestation using the GEE platform to process Sentinel-1 data from nearly 6000 locations across the Brazilian Amazon. Nevertheless, as described by [53], GEE too has limitations. Despite its powerful service offered to scientists and researchers to analyze such planetary-scale repository of satellite imagery and geospatial datasets, the on-demand work mode restricts the maximum run time to 5 minutes [53]. In other words, it is inadequate for operational level use unless subscribed [54].

2.2 An Overview Of U-Net

In order to improve the disturbances classification in tropical forests, it is essential to understand which algorithm works best in a given scenario. The DL is one of the most widely studied computer visions and is often used for semantic segmentation on very high-resolution optical imagery [55]. In particular, deep learning aims to automatically extract multi-layer feature representations from data, and it has been successfully applied to target recognition [56].

Based on a literature review by [57], U-Net and SegNet are other examples of existing deep learning algorithms proven to be helpful in deforestation studies. The U-Net algorithm was about 11.5 percent more accurate for detecting forest and non-forest land when compared to the SegNet algorithm [57].

First proposed by [58], U-Net is fast and accurate in segmenting images. It has a U-shaped structure and one of the first popular architectures based on a fully convolutional network (FCN) [44]. U-Net is an encoder-decoder architecture. The encoder is the first half of the U-Net that downsamples the input feature maps through convolutional layers. By comparison, the decoder is the second half of the U-Net, aiming to recover the image's details by upsampling input feature maps and cross-layer connections between the corresponding encoder feature maps of the exact resolution. Finally, the anticipated class is represented by the final feature map. Another advantage of the U-Net is that it can work with fewer training sets and still produce higher segmentation accuracy [59].

Due to the qualities mentioned above, the U-Net has been one of the most effective deep neural networks (DNN) for RS applications. The U-Net was used in [60] to map forest types and tree species in the Brazilian rainforest using high spatial resolution imagery, obtaining over 95 per cent accuracy for most classes. Also, [61] showed the potential of DNN architecture for LULC mapping over RS imagery by proposing a Residual U-Net to recognize roads on high-resolution imagery, reaching roughly 90 percent accuracy.

As we will see in the following section, our work takes advantage of the U-Net encoder-decoder structure and how it represents two outcome variations of this DNN network for forest and deforestation (non-forest) mapping tasks, allowing it for interpretation not just spectral but also temporal information.

2.3 Orfeo ToolBox TensorFlow Application

This subsection introduces the Orfeo Toolbox TensorFlow (OTBTF) application, which focuses on making deep learning techniques accessible to RS analysts with only a few lines of source code and user-oriented process objects. It was developed by [62] and consists of configurable building blocks to perform spatial and multi-temporal DL-based real-world RS data analysis. OTBTF integrates Python and C++ with three basic steps to perform the deep learning tasks: Patches sampling, TensorFlow model train, and TensorFlow model serve. OTBTF is distributed as free and open-source software under the GNU General Public License version 3.0 or later, running on Docker software and installed on multiple platforms (e.g., Windows, Mac OS X and Linux). Using TensorFlow, this application is highly scalable to process large volumes of data while being flexible and extendable to execute the entire deep learning-based analysis cycle [62]. OTBTF also provides evaluation metrics reports such as Precision, Recall, F-Score, Kappa Index, OA, and Confusion Matrix. In the following sections, we will construct a simple U-Net model and demonstrate how to employ OTBTF features in this study.

2.4 The Temporal Resolution Of SAR Data

Active SAR sensors benefit from polarization channels, as opposed to passive optical sensors, which benefit from multi-spectral bands, [63]. SAR images are formed from the measurement of amplitude and phase of the backscattered signal. In the past, phase differences are required to indicate land deformation, whereas amplitude is used to identify the land cover classification and changes. For instance, phase and amplitude combinations using ERS SAR data to map vegetation cover and monitor changes in forest environments [64]. This method is still in use today. Multi-temporal acquisitions, independent of amplitude or phase, have recently been used to improve accuracy while reducing the negative effects (e.g., speckle noise) seen with single-date acquisitions. The authors in [24] employed the concept using interferometric short-time-series data from Sentinel-1 as features for the machine learning RF classifier and achieved an accuracy of 85%. In another study [56], classification accuracy of the disturbed forest was improved up to 25% when using time-series SAR instead of using only one data acquisition.

A pair of Sentinel-1A/1B missions have a 6-day revisit period when image acquisitions are undertaken in both ascending and descending directions [65]. With regular SAR observations and rapid product delivery products, either Single Look Complex (SLC) and/or Ground Range Detected (GRD), is potential for large-scale ground deformation measurements has gotten considerably more attention in recent years. In SAR interferometry, two identical path and orbit images are required for coregistration methods (e.g. a pair of ascending-ascending or descending-descending) because a single SAR image has no practical use [66]. This method is very beneficial since it enables the monitoring of terrain changes caused by earthquakes and landslides. [66]. However, there are only few studies examined the

potential for combining polarimetric information from ascending and descending data sets for land cover mapping or classification, except some studies have examined the use of ascending and descending to create a more accurate digital elevation model (DEM) data set in order to overcome inherent geometric distortions. For example, [67] determine the optimum incidence angle of TanDEM-X⁷ SAR data by performing a simple weighted fusion of ascending and descending data, resulting in an 8% reduction of error standard deviation for urban classes. As such, in this study, we undertake experiments in both ascending and descending directions on time series of GRD data sets in order to generate a comprehensive set of feature maps for our U-Net model.

3.0 EXPERIMENTAL DESIGN

The methodology of this study is divided into seven subsections as shown in Fig. 1: **i.** SAR data preparation; **ii.** SAR data pre-processing; **iii.** False-colour image creation; **iv.** Sample selection; **v.** Building the U-Net model; **vi.** Inference analysis; and, **vii.** Comparison with random forest. Similar to [34], the study area is located between 102°16'6" E, 3°54'39" N and 102°20'58" E, 4°28'10" N as shown in Fig. 2. HSK Yong is surrounded by agricultural areas such as palm oil and rubber. The topography of the surrounding area consists of thick forests, hills, and nearby to two rivers, namely Sungai Jelai and Sungai Tembeling. However, since 2017, it was reported that HSK Yong had engaged in aggressive loggings activities, which affecting the nearby villagers [68]. After reviewing the recent Sentinel-2 imaging over the HSK Yong region dated 8th February 2020, no new land changes have occurred in the logging areas, indicating that this site is suitable for our experiment.

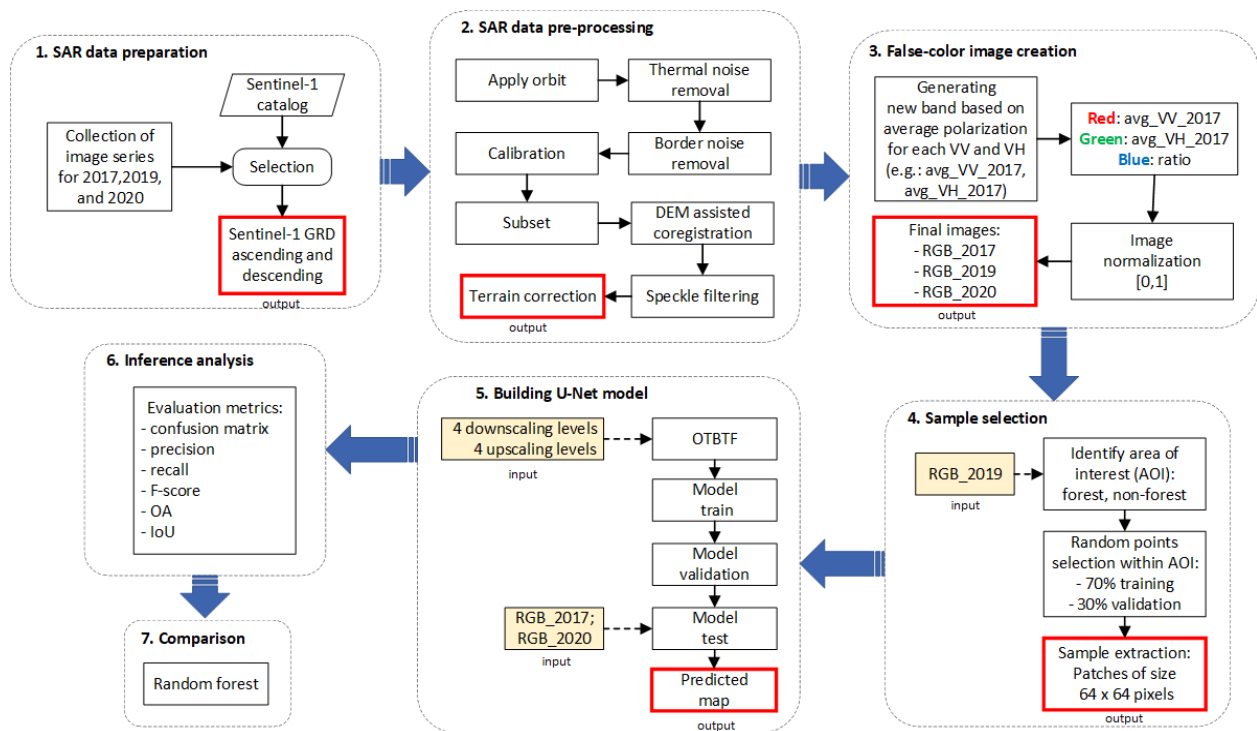


Fig. 1: Overall flow of the experiment design that consists of seven subsections. i. SAR data preparation; ii. SAR data pre-processing; iii. False-color image creation; iv. Sample selection; v. Building the U-Net model; vi. Inference analysis; and vii. Comparison with random forest.

⁷ TanDEM-X is an abbreviation for TerraSAR-X add-on for Digital Elevation Measurement, and it is operated by German Earth Observation.

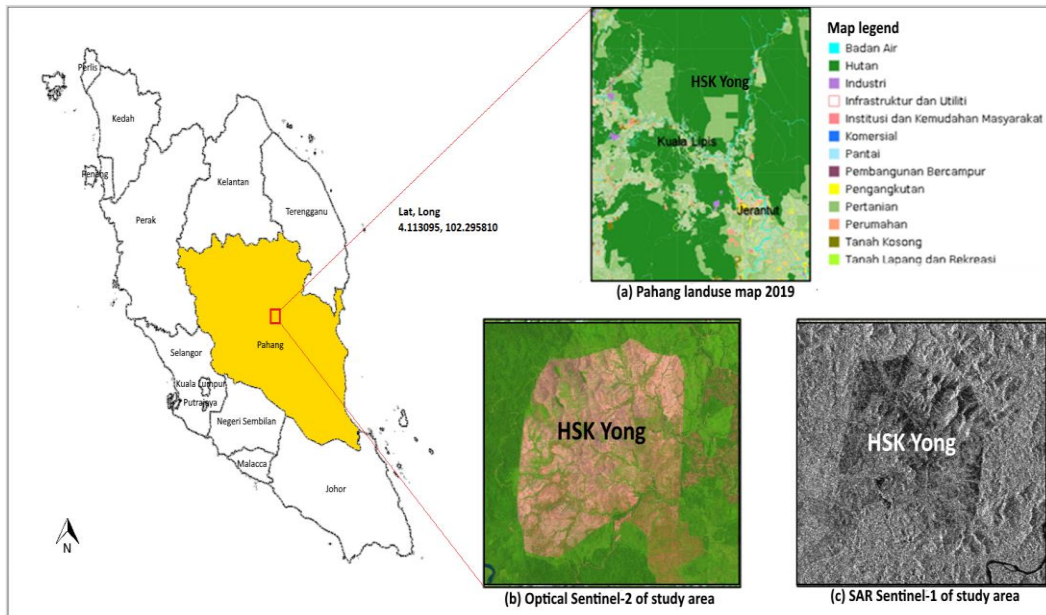


Fig. 2: HSK Yong location with overview, (a) Pahang land use map; (b) Sentinel-2 image; (c) Sentinel-1 image. Source [34].

3.1 SAR Data Preparation

Five images from each years of 2017, 2019, and 2020 were downloaded from the Alaska Satellite Facility's (ASF) data search page [69], in Level-1 GRD format with ascending and descending orbits as shown in Table 1. Three different time frames were used to express the following deforestation conditions: before, during, and after of the study area. We retained a six-day interval between each image for homogeneity purposes, except for 2017 due to image unavailability.

Table 1: List of Sentinel-1 data acquisitions to cover the area of interest

Satellite	Acquisition	Orbit	Track	Final stacked image
Sentinel-1A/1B in Level-1 GRD	3/7/2017	descending	91	RGB_2017
	9/7/2017	ascending	172	
	15/7/2017	descending	91	
	2/8/2017	ascending	172	
	8/8/2017	descending	91	
	6/1/2019	descending	91	RGB_2019
	12/1/2019	ascending	172	
	18/1/2019	descending	91	
	24/1/2019	ascending	172	
	30/1/2019	descending	91	
	5/7/2020	ascending	172	RGB_2020
	11/7/2020	descending	91	
	17/7/2020	ascending	172	
	23/7/2020	descending	91	
	29/7/2020	ascending	172	

3.2 SAR Data Pre-Processing

There are two modifications made to the prior study in this section: addition of a DEM-assisted coregistration (DAC) technique and multitemporal speckle filter technique. The common coregistration methods used in the SAR interferometry includes coregistration based on a double cross-correlation of images and coregistration based on orbital data and DEM [70]. The former requires an image with a similar orbit and track, which incompatible with the current study. Moreover, the areas without elevation were masked based on DEM data. We relied on the Copernicus DEM for the DEM data at a resolution of 30m because there was no local DEM data available in the study area.

Besides, this global dataset has been made available for download by the European Space Agency (ESA) and is publicly available. The DEM's accuracy is about 4m vertically and 6m horizontally [71].

The multitemporal speckle filter technique used in this study followed the recommendation of [72] that the Boxcar filter outperforms other methods in removing speckle noise while maintaining the edges of objects' visual integrity of the image. The Boxcar filter was set at 3x3 pixels. Finally, each image was resampled to 10m from 30m and terrain-corrected using a well-known coordinate projection, i.e., EPSG 3857, to achieve the final outputs. As a 'good practice', we visually assessed the final outputs from this subsection by overlaying it with Google Earth Pro.

3.3 False-Color Image Creation

Previously, we constructed false-colour RGB composites based on Principal Component Analysis (PCA) through Gray-Level Co-occurrence Matrix (GLCM) data from a single date. Now that we dealt with multi-temporal data, a new band/variable was constructed based on temporal means. In other words, given combined ascending and descending image collections, the mean VV and mean VH were calculated for 2017, 2019, and 2020 respectively. The approach mentioned above was thoroughly discussed in [73]. Afterwards, the following image was created based on the following: mean VV for the red channel, mean VH for the green channel, and blue channel for the ratio between mean VV and mean VH.

Normalization was applied to ensure that each pixel value falls within the range of 0 to 1. Smaller pixel values can help speed up the learning process in some cases [44]. Subsequently, the final versions of RGB 2017, RGB 2019, and RGB 2020 were exported to the '.tif' format with a dimension of 1581x1888 pixels and readied for the following phase.

3.4 Sample Selection

As shown in Fig. 3, we positioned the grid's centroid (within the non-forest AOI) on top of the RGB 2019 image. Then, through *PatchExtraction* from OTBTF, we extracted a collection of image patches with size of 64x64 pixels (randomly) and divided into two groups: 70 per cent for training and 30 per cent for validation. As a clarification, the sampling strategy was based on that described in [44], namely random selection. The red dot in Fig. 3 corresponded to the training sample, while the blue dot corresponded to the validation sample. Finally, all patches were validated by cross-referencing against the Pahang land use map and Google Earth Pro. Please note that our image annotation method was referred to as the semantic labelling technique [74]. Our objective was to assign the non-forest class to each pixel within an AOI area. Thus, any patches that did not fall under the AOI were regarded as a forest class.

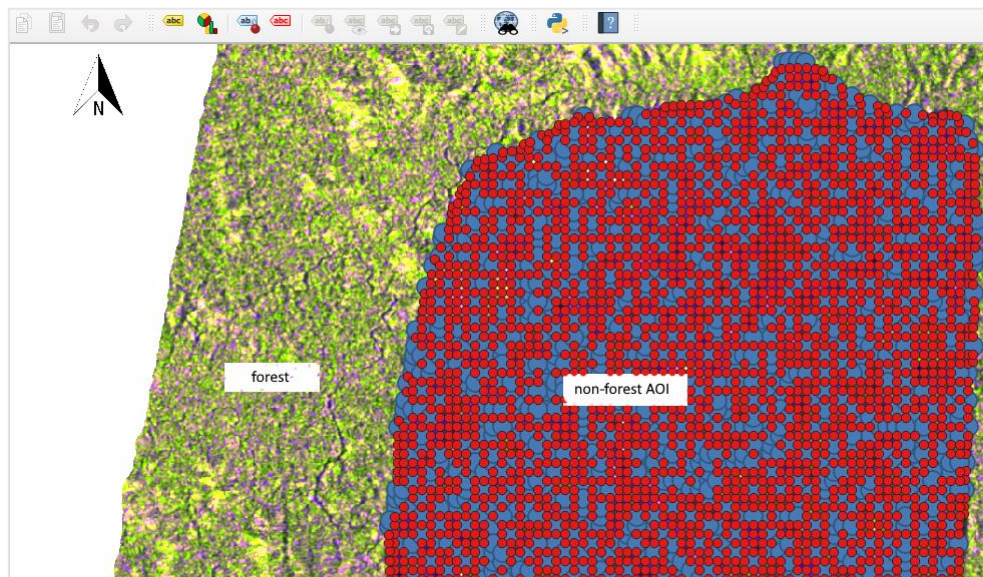


Fig. 3: A snapshot of the QGIS software (version 3.10) demonstrates a part of the working area used in the sample selection process. The sample selection process was based on the centroid of the vector grid. Each grid pixel is 96x96 meters in size to cover the designated AOI of the non-forest class. Red dot refers to training sample, while blue dot refers to validation sample.

3.5 Building The U-Net Model

The U-Net architecture employed in this study to map deforestation is illustrated in Fig. 4. Our concept is straightforward and easy to implement utilizing the OTBTF framework. First, the downscaling levels were composed of four convolutional layers with stride 2, followed by a rectified linear unit (ReLU). Next, the upscaling levels were composed of four convolutional layers transposed with stride 2, followed by a ReLU. Finally, the last layer comprises two neurons: one for the forest class (represent the background) and another for the non-forest class.

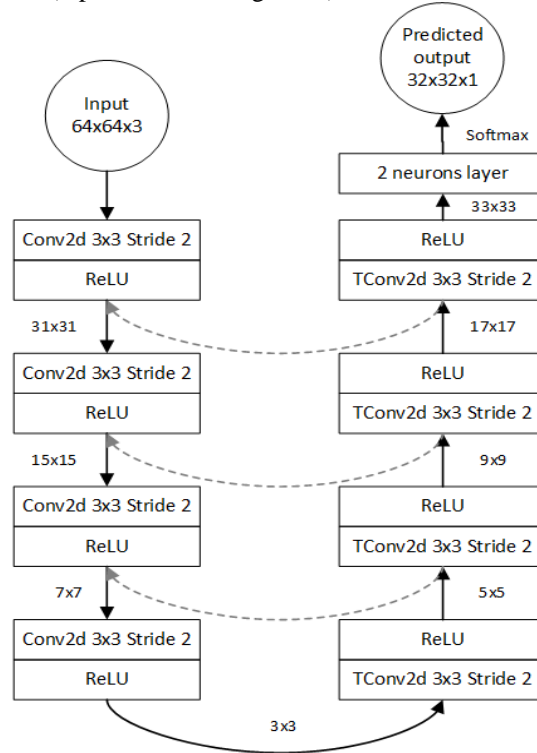


Fig. 4: Simple U-Net with 4 downscaling/4 upscaling levels, which was then programmed in Python.

After compiling the model in Python, training began with 20,5312 patches of size 64x64x3 pixels as inputs. In contrast to classical machine learning approaches, *TensorflowModelTrain* from OTBTF hides the complexity of the training and offers an easy-to-use interface to train our model. The following hyper-parameters were used: Learning rate:0.00001; Epoch number:100; Batch size:100; Optimizer: Adam. Similarly, these hyper-parameters were also used to validate the model of 88,000 patches, where training and validating operations were ran simultaneously. Afterwards, *TensorflowModelServe* was used to test the trained model against RGB 2017 and RGB 2020 images to generate predicted deforestation maps as outcomes.

3.6 Inference Analysis

Several evaluation measures from the OTBTF were used in our inference analysis namely, precision, recall, F-score, Kappa index, and OA. However, interpreting these assessment measurements toward unbalanced classes for semantic segmentation can be inaccurate due to a high fraction of pixels from the background compared to other classes [44]. Thus, the F-score is employed because it represents a compromise between precision and recall [44].

IoU is a viable choice because it is widely used for evaluating models based on semantic segmentation [75]. Specifically, the IoU formula (1) is defined as:

$$IoU = \frac{\text{true positive}}{\text{true positive} + \text{false positive} + \text{false negative}} \quad (1)$$

The balance of 30 percent image patches (a total for the validation samples is 88,000 patches) were used to assess the F-score and IoU and the findings is presented in the results and analysis section.

3.7 Comparison With Random Forest

RF is a supervised machine learning technique for classification. This technique was originally introduced by [76] for the machine learning group to overcome the weaknesses of a single decision tree. Since then it has gained popularity among the RS community in classifying remotely sensed imagery, due to ease of parametrization, speed and accuracy [77]. RF model has only two tuning parameters [78]: the number of classification trees to be produced (k) and the number of predictor variables used at each node (m). This study used RF to compare the outcomes from the U-Net model; performance as well as visualized analysis. To use RF, we started with feature labels as our terrain truth labelling. Polygons were drawn to represent the forest and non-forest areas using the RGB 2019 image as shown in Fig. 5. Since ground-truth fieldwork sample data were not available, all polygons (covered forest and non-forest areas) were digitized and labelled accordingly (Pahang 2019 land use map as reference). No polygons were overlapped during the digitization process and verified using Google Earth Pro. Then, the Sentinel Application Platform (SNAP) software (version 8.0) was used to perform supervised classification on 10,000 training samples (5,000 forests; 5,000 non-forests) and 100 trees. Finally, the results were analyzed and presented in Table 2.

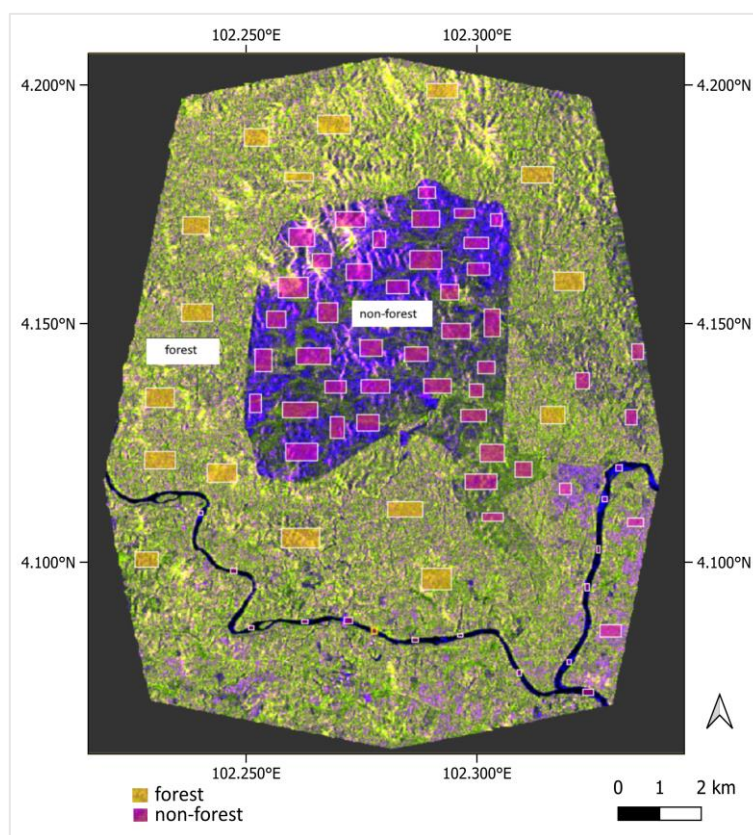


Fig. 5: Terrain truth labelling (polygons were digitized) of the area of interest as inputs for random forest using SNAP.

4.0 RESULT AND ANALYSIS

The outputs of five subsections (SAR data preparation; SAR data pre-processing; False-color image creation; Sample selection; Building the U-Net model) are visualized in Fig. 9. As shown in the SAR data preparation subsection, each imagery data was slanted to the side due to geometrical distortion. Additionally, some images of the east coast of peninsular were inverted and rotated at 180 degrees. The distortion occurred because the data was acquired using the SAR system's side-look geometry and projected to ground range using an Earth ellipsoid model [43]. The corrections of the terrain were performed during SAR data pre-processing subsection, after the outputs were subset to AOI, to ensure that the geometric representation of the image is as close as possible to the surface of the earth. It can be observed that the newly processed imagery data has been shifted, and characteristics began to take on a more streamlined appearance. Even though few studies have explored DAC using Level-1 GRD data for deforestation mapping, we can reasonably assume that this approach was justified due to the results seen in this subsection. Next, under the false-color image creation subsection, the outputs were instrumental in establishing the foundation for our U-Net-based semantic segmentation. As explained in subsection 2.1, RGB is needed for distinguishing across classes.

The classes identified were water bodies, forest lands, deforestation activities areas and agricultural lands. These classes served as the foundation for subsequent sample selection procedure. In the sample selection subsection, all classes were grouped as follows, forest and non-forest where non-forest was comprised by deforestation activities, water bodies, and agricultural lands (see Fig. 6). The samples were generated as square patches of 64x64 pixels, along with their labelling, where code '0' indicates forest (color in black) and code '1' indicates non-forest (color in white). A total of 70% of the patches were used to train the U-Net model and output predicted maps (i.e., predicted map for 2017 and predicted map for 2020) presented under the U-Net model's subsection. In addition, the multi-temporal imaging data utilized in this model proved that the semantic segmentation process is more capable of dealing with speckle noise effects than our earlier study in [34]. Overall, the predicted map displayed promising ability in distinguishing between non-forest and forest, suggesting the work may serve as a foundation for future scholars to build upon and improve.

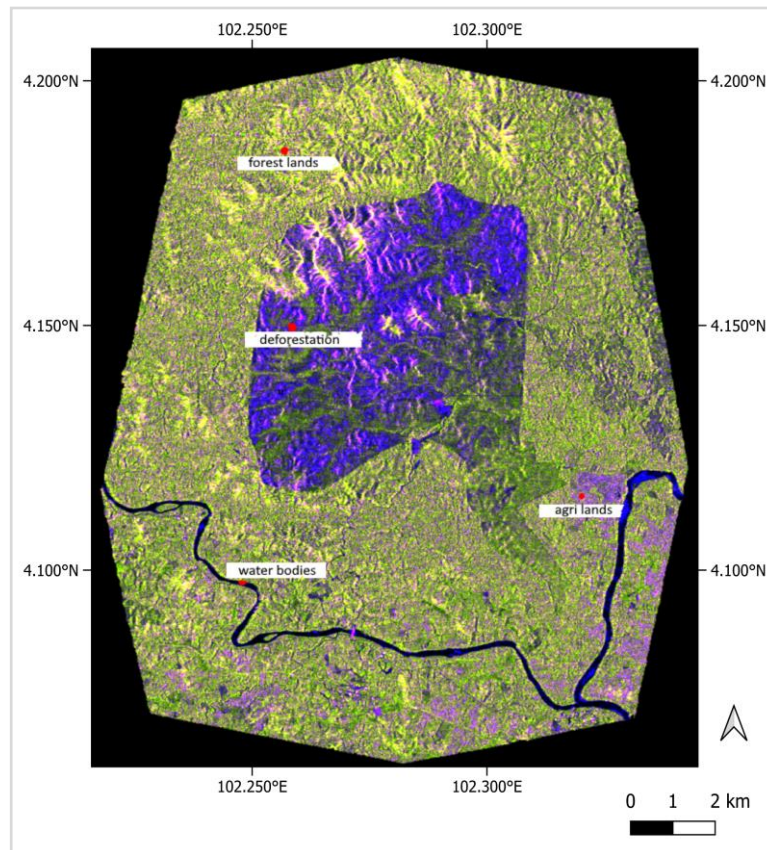


Fig. 6: This is the output from the false-color RGB creation subsection. As can be seen, this method allows the study to identify several classes such as forest lands, deforestations area, water bodies, and agricultural lands.

Two confusion matrixes each for U-Net and RF are generated to express the classification accuracy (see Fig. 7). The predicted labels are shown on the x-axis while the true labels are shown on the y-axis. True negative (TN) is in the upper left corner, true positive (TP) is in the lower right corner, false positive (FP) is in the upper right corner, and false negative (FN) is in the lower left corner. Overall, the U-Net attained a TP value of 0.99, RF attained a TP of 0.79. As comparison with [34], U-Net performed significantly better than CNN. Thus, we can infer that U-Net can accurately predict the non-forest class throughout the experiment based on TP alone.

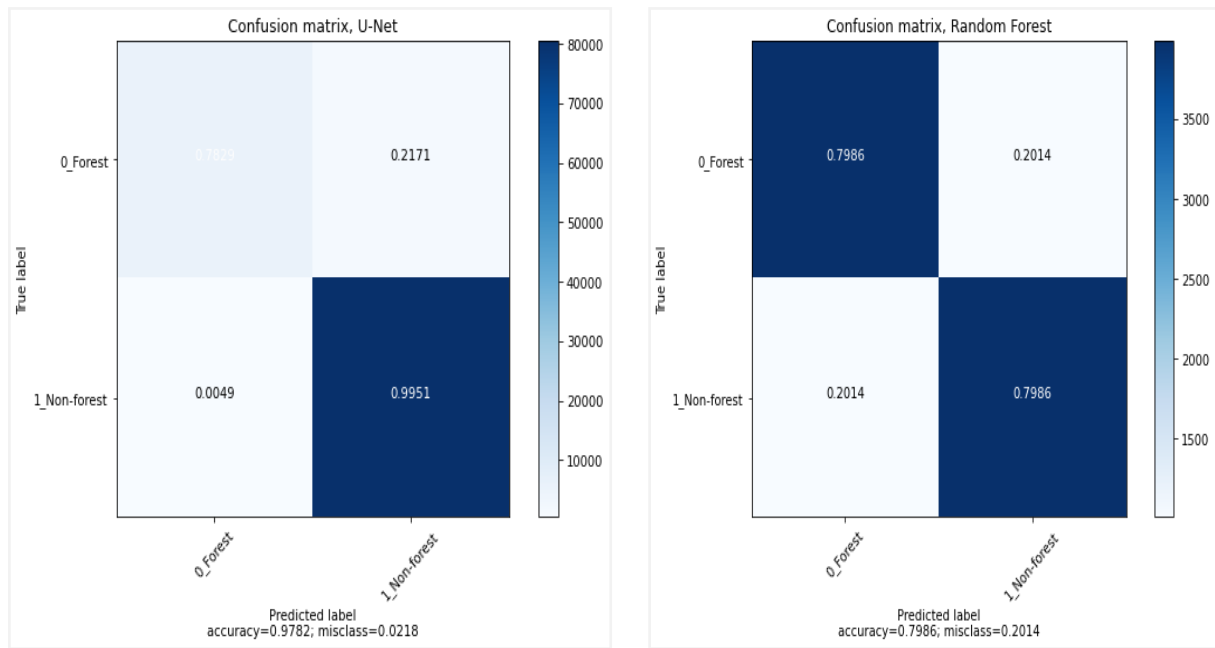


Fig. 7: Confusion matrix plot between U-Net and random forest.

Table 2 shows the Precision, Recall, F1-score, OA, and IoU to evaluate the U-Net capabilities and effectiveness in segmenting each targeted class. The mean F1-score and IoU are greater than 0.8, suggesting that multi-temporal SAR bring better results than [34]. Also, the U-Net model has an overall accuracy of 0.98 compared to 0.82 in [34]. When comparing forest and non-forest classes, the non-forest class consistently has the Precision, Recall, and F1-score values higher than 0.9. This most likely related to our sample selection procedure (semantic segmentation) differs from the prior study (patch-based).

Table 2: Evaluation metrics of the U-Net and random forest for comparison.

	U-Net		RF	
	Forest	Non-forest	Forest	Non-forest
Precision	0.9057	0.9897	0.7772	0.8236
Recall	0.8468	0.9940	0.8372	0.7600
F1-score	0.8753	0.9919	0.8061	0.7905
OA	0.9782		0.7986	
IoU mean	0.9930		-	

Fig. 8 depicts the map output between U-Net and RF. As expected, U-Net outperforms random forest with significant visualization improvements. On the other hand, the OA for RF was significantly lower at 0.79, as shown in Table 2. The F1-score of the forest class was much higher than that of the non-forest class in the RF, which contradicted the U-Net. The mean IoU is not measured for RF as the measurement is better suited for segmentation-based semantic analysis [75]. One of the reasons for RF poorer classification performance between forest and non-forest is due to the speckle noise effects. Regarding this, a study by [79] could serve as an explanation, as they had tested the effect of various simulated noise levels (i.e., 10%, 20%, and 30%) on RF classifier and discovered that when noise levels increased, the RF classifier's classification accuracy decreased. Another study by [80] investigated the impact of salt-pepper noise on classification accuracy in remotely sensed data between several different ML classifiers (e.g., RF, SVM, and back-propagation neural network). They revealed that RF outperformed all of the classifiers in salt-pepper noise added image classification. Thus, given the points above, U-Net-based semantic segmentation would be a preferable alternative to CNN and RF for mapping deforestation in Peninsular Malaysia.

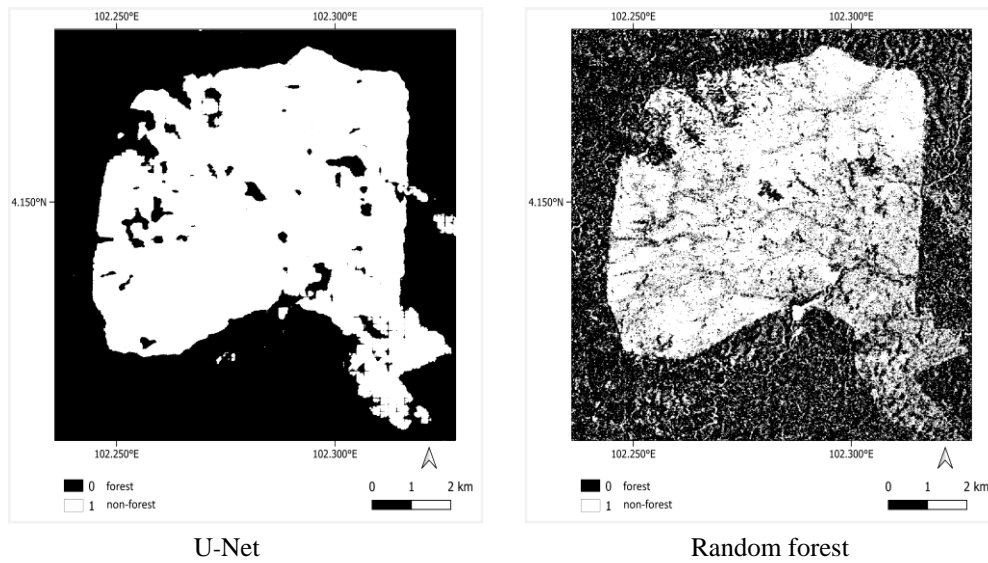


Fig. 8: Visualize comparison between U-Net and random forest of the predicted map. On the left, U-Net predicted the probabilities of deforestation area by providing a local region (patch) around that pixel in the input, as opposed to the result from the random forest. Color in black is forest, while color in white is non-forest.

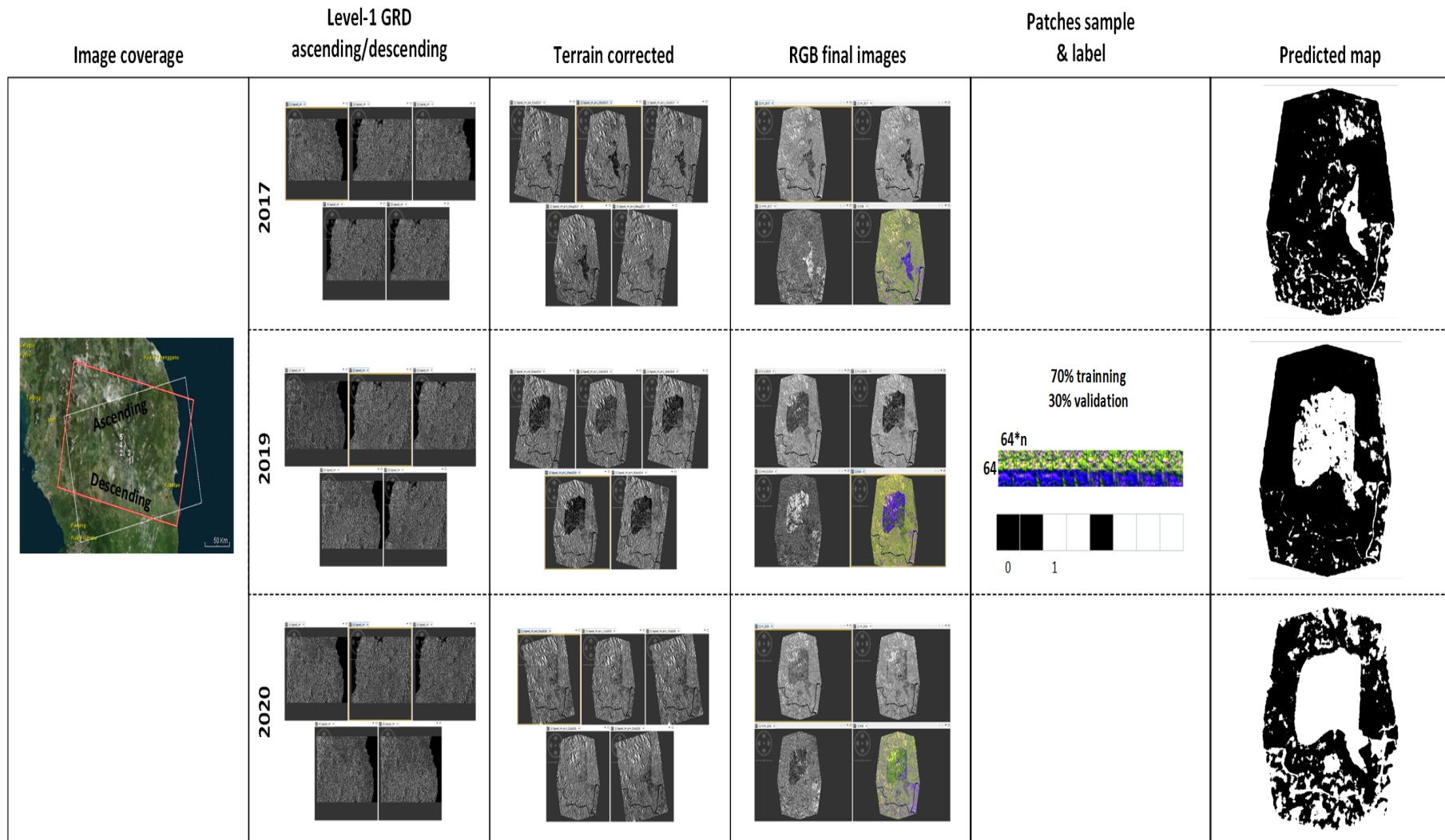


Fig. 9: Five different outputs from five subsections process corresponding to Fig. 1. Note that, in the Level-1 GRD ascending/descending section and the terrain corrected section, the total images are 10 (consisting of VV and VH channels) for every five different dates in 2017, 2019, and 2020. However, only the VH channel is shown.

5.0 DISCUSSION

This study presents an end-to-end process that is geared toward beginners and operational usage. In particular, this study focuses on multi-temporal Sentinel-1 SAR, simplicity and speed in order to provide timely, accurate and relevant information for HSK deforestation mapping. The open-source software (OSS) such as SNAP, QGIS, OTBTF, and Python were also incorporated into this work. Previous study by [18] used Carnegie Landsat Analysis System-Lite (CLASlite) algorithm to map forest cover and forest disturbance in Peninsular Malaysia using optical and SAR data. The study regarded land covered in palm oil plantations as an indicator of forest disturbance, but failed to distinguish forest vegetation, oil palm and rubber trees. Each time a new class was created, new thresholds must be developed. A study by [81] used a different approach to identify oil palm land cover in Peninsular Malaysia, and the approach was based on machine learnings and GEE. However, implementing machine learning optimization utilizing GEE over a vast area proved challenging despite the encouraging results [81]. In this context, the issue of how to employ exact, current, and up-to-date procedures would remain unresolved. The work presented in our study introduced the semantic segmentation using a U-Net like architecture, a popular model targeting semantic segmentation of images. A simple model was developed and applied to identify forest and non-forest from the entire multi-temporal SAR image, with no size constraints and in a reasonable amount of time. As previously established, semantic segmentation makes use of U-Net and preserve the spatial resolution of the output compared to the patch-based approach. However, since the RF classifier is simple to build using SNAP, it is often used for comparison with DL in prior studies [36], [37] despite the overall accuracy results did not match those of the U-Net. Therefore, our study would be preferable over RF with easy implementation of DL for automated deforestation mapping system using SAR imagery data while maintain a high classification accuracy.

There are several aspects of this study can be further improved: **i.** Consider various alternatives to the Boxcar filter for pre-processing Sentinel-1 data. Finding the optimal speckle filtering method for Sentinel-1 data will result in an increased capacity for comprehending and analyzing images under a variety of conditions. For example, SAR2SAR a semi-supervised despeckling technique for SAR images based on deep learning [82]. **ii.** Currently, findings were validated through eye inspections and cross-checking against the Pahang land use map 2019, Sentinel-2, and Google Earth Pro. This inspection is sufficient for validation [34] but the ground-truth fieldwork can offers detailed insight which not available from SAR images. **iii.** As previously stated in subsection 2.1, to obtain an acceptable result using semantic segmentation, patches of images must be completely annotated, that is, each pixel in the image must be labelled with the appropriate class. According to [83], knowledge transfer from one supervised method (e.g. RF) to semantic segmentation is possible. This might be beneficial in addressing the issue of labelling training data in huge quantities.

6.0 CONCLUSION

Forests are a critical component of environmental and economic sustainability, immediate action is required to protect this natural resource for the vitality of the ecosystem and avert environmental disasters. From the experimental results, the U-Net model and multi-temporal Sentinel-1 in Level-1 GRD produced significant improvement with IoU of 0.993 and OA of 0.984 compared to the previous study. Further, U-Net outperformed RF in terms of visualized analysis. This study can be extended by fusing Sentinel-1 and Sentinel-2 data for image restoration. This new experiment could be accomplished by using a two-branch downscaling technique that can accept inputs from both SAR and optical data sources. The two feature maps obtained could potentially be concatenated to create cloud-free artificial optical images from SAR input data, which would help enhance forest monitoring activities, particularly in tropical countries like Malaysia. After all, if avoided deforestation is not a good measure of sustainability impact, what would be better?

Finally, breakthroughs in DL technologies for RS will be feasible only through close collaboration between government agencies, research institutes, universities, and the private sector. This is especially true with SAR. As such, we encourage future collaborative initiatives to explore DL-powered big data analytics that are more comprehensible and reproducible.

ACKNOWLEDGMENT

This study was fully supported by University Kebangsaan Malaysia. It was funded by the Public Service Department, Government of Malaysia. The authors would like to thank the Alaska Satellite Facility from University of Alaska for providing Sentinel-1 images, European Space Agency for providing Sentinel-2 images, and lastly, the Malaysian Department of Town and Country Planning (PLANMalaysia) for providing land use data via their I-Plan online site. The authors declare no conflict of interest.

REFERENCES

- [1] Nobel Foundation, "Al Gore – Facts," *Nobel Prize Outreach AB 2021*. <https://www.nobelprize.org/prizes/peace/2007/gore/facts/> (accessed 04th July, 2021).
- [2] A. Gore, *An inconvenient truth: The planetary emergency of global warming and what we can do about it*. Emmaus, PA, US: Rodale Press, 2006.
- [3] D. Carrington, N. Kommenda, and C. Levett, "One football pitch of forest lost every second in 2017, data reveals," *The Guardian*, 2018.
- [4] C. Mooney, B. Dennis, and J. Muyskens, "Global forest losses accelerated despite the pandemic, threatening world's climate goals," *The Washington Post-Climate and Environment*, 31st March, 2021.
- [5] M. Miyamoto, "Poverty reduction saves forests sustainably: Lessons for deforestation policies," *World Dev.*, vol. 127, p. 104746, Mar. 2020, doi: 10.1016/j.worlddev.2019.104746.
- [6] H. Kamaruddin, R. Md Khalid, D. I. Supaat, S. Abdul Shukor, and N. Hashim, "Deforestation and Haze in Malaysia: Status of Corporate Responsibility and Law Governance," Nov. 2016, pp. 374–383, doi: 10.15405/epsbs.2016.11.02.34.
- [7] M. Miyamoto, M. Mohd Parid, Z. Noor Aini, and T. Michinaka, "Proximate and underlying causes of forest cover change in Peninsular Malaysia," *For. Policy Econ.*, vol. 44, pp. 18–25, Jul. 2014, doi: 10.1016/j.forpol.2014.05.007.
- [8] B. Nambiappan, "Malaysia: 100 Years Of Resilient Palm Oil Economic Performance," *J. Oil Palm Res.*, pp. 13–25, Apr. 2018, doi: 10.21894/jopr.2018.0014.
- [9] H. Rohiman, "Sustainability and Palm Oil," *New Straits Times*, 19th January, 2020.
- [10] M. N. H. M. Noor, R. Kadir, and S. Muhamad, "ILLEGAL LOGGING AND FOREST OFFENCES IN PENINSULAR MALAYSIA: PERCEIVED OPPORTUNITY FACTORS," *J. Nusant. Stud.*, vol. 5, no. 2, pp. 86–102, Jun. 2020, doi: 10.24200/jonus.vol5iss2pp86-102.
- [11] S. Managi, J. Wang, and L. Zhang, "Research progress on monitoring and assessment of forestry area for improving forest management in China," *For. Econ. Rev.*, vol. 1, no. 1, pp. 57–70, Apr. 2019, doi: 10.1108/FER-04-2019-0012.
- [12] J. Li, Y. Pei, S. Zhao, R. Xiao, X. Sang, and C. Zhang, "A Review of Remote Sensing for Environmental Monitoring in China," *Remote Sens.*, vol. 12, no. 7, p. 1130, Apr. 2020, doi: 10.3390/rs12071130.
- [13] A. Rahman, "Application of Geospatial Technology as Tool for Effective Forest Management in Peninsular Malaysia," 2014.
- [14] ESA, "SAR Handbook," 2014. <https://earth.esa.int/handbooks/asar/CNTR1-1-5.html> (accessed 07th September, 2020).
- [15] MYSA, "MYSA-Background," 2020. <https://www.mysa.gov.my/background/> (accessed 30th June, 2021).
- [16] Harian Metro, "Penggunaan FMRS berkesan," *Harian Metro*, Dec. 18, 2016. <https://www.hmetro.com.my/mutakhir/2016/12/189886/penggunaan-fmrs-berkesan> (accessed Jul. 01, 2021).
- [17] A. M. Durieux *et al.*, "Monitoring forest disturbance using change detection on synthetic aperture radar imagery," vol. 1113916, no. September 2019, p. 39, 2019, doi: 10.1117/12.2528945.
- [18] N. E. Mohd Najib and K. D. Kanniah, "Optical and radar remote sensing data for forest cover mapping in Peninsular Malaysia," *Singap. J. Trop. Geogr.*, vol. 40, no. 2, pp. 272–290, May 2019, doi: 10.1111/sjtg.12274.
- [19] N. E. Najib and K. D. Kanniah, "Optical and radar remote sensing data for forest cover mapping in Peninsular Malaysia," *Singap. J. Trop. Geogr.*, vol. 40, no. 2, pp. 272–290, May 2019, doi: 10.1111/sjtg.12274.

- [20] A. Bouvet, S. Mermoz, M. Ballère, T. Koleck, and T. Le Toan, "Use of the SAR shadowing effect for deforestation detection with Sentinel-1 time series," *Remote Sens.*, 2018, doi: 10.3390/rs10081250.
- [21] J. Ruiz-Ramos, A. Marino, C. Boardman, and J. Suarez, "Continuous Forest Monitoring Using Cumulative Sums of Sentinel-1 Timeseries," *Remote Sens.*, vol. 12, no. 18, p. 3061, Sep. 2020, doi: 10.3390/rs12183061.
- [22] I. Borlaf-Mena, M. Santoro, L. Villard, O. Badea, and M. Tanase, "Investigating the Impact of Digital Elevation Models on Sentinel-1 Backscatter and Coherence Observations," *Remote Sens.*, vol. 12, no. 18, p. 3016, Sep. 2020, doi: 10.3390/rs12183016.
- [23] M. Gašparović and D. Dobrinić, "Comparative Assessment of Machine Learning Methods for Urban Vegetation Mapping Using Multitemporal Sentinel-1 Imagery," *Remote Sens.*, vol. 12, no. 12, p. 1952, Jun. 2020, doi: 10.3390/rs12121952.
- [24] A. Pulella, R. Aragão Santos, F. Sica, P. Posovszky, and P. Rizzoli, "Multi-Temporal Sentinel-1 Backscatter and Coherence for Rainforest Mapping," *Remote Sens.*, vol. 12, no. 5, p. 847, Mar. 2020, doi: 10.3390/rs12050847.
- [25] B. Brisco, A. Schmitt, K. Murnaghan, S. Kaya, and A. Roth, "SAR polarimetric change detection for flooded vegetation," *Int. J. Digit. Earth*, vol. 6, no. 2, pp. 103–114, Mar. 2013, doi: 10.1080/17538947.2011.608813.
- [26] P. R. Coppin and M. E. Bauer, "Digital change detection in forest ecosystems with remote sensing imagery," *Remote Sens. Rev.*, vol. 13, no. 3–4, pp. 207–234, Apr. 1996, doi: 10.1080/02757259609532305.
- [27] K. Nackaerts, K. Vaesen, B. Muys, and P. Coppin, "Comparative performance of a modified change vector analysis in forest change detection," *Int. J. Remote Sens.*, vol. 26, no. 5, pp. 839–852, Mar. 2005, doi: 10.1080/0143116032000160462.
- [28] Z. Sun, H. Geng, Z. Lu, R. Scherer, and M. Woźniak, "Review of Road Segmentation for SAR Images," *Remote Sens.*, vol. 13, no. 5, p. 1011, Mar. 2021, doi: 10.3390/rs13051011.
- [29] D. E. Kislov, K. A. Korznikov, J. Altman, A. S. Vozmishcheva, and P. V. Krestov, "Extending deep learning approaches for forest disturbance segmentation on very high-resolution satellite images," *Remote Sens. Ecol. Conserv.*, p. rse2.194, Jan. 2021, doi: 10.1002/rse2.194.
- [30] A. Mazza, F. Sica, P. Rizzoli, and G. Scarpa, "TanDEM-X Forest Mapping Using Convolutional Neural Networks," *Remote Sens.*, vol. 11, no. 24, p. 2980, Dec. 2019, doi: 10.3390/rs11242980.
- [31] CAMP 21, "Fifth International Conference on Information Retrieval and Knowledge Management," *Malaysian Society of Information Retrieval and Knowledge Management*, 2021. <https://camp21.pecamp.org/> (accessed 07th July, 2021).
- [32] J. Irvin *et al.*, "ForestNet: Classifying Drivers of Deforestation in Indonesia using Deep Learning on Satellite Imagery," Nov. 2020, [Online]. Available: <http://arxiv.org/abs/2011.05479>.
- [33] U. Sivarajah, M. M. Kamal, Z. Irani, and V. Weerakkody, "Critical analysis of Big Data challenges and analytical methods," *J. Bus. Res.*, vol. 70, pp. 263–286, Jan. 2017, doi: 10.1016/j.jbusres.2016.08.001.
- [34] M. A. A. Wahab, E. S. M. Surin, and N. M. Nayan, "An Approach to Mapping Deforestation in Permanent Forest Reserve Using the Convolutional Neural Network and Sentinel-1 Synthetic Aperture Radar," in *2021 Fifth International Conference on Information Retrieval and Knowledge Management (CAMP)*, Jun. 2021, pp. 59–64, doi: 10.1109/CAMP51653.2021.9498144.
- [35] S. Y. Lee, B. A. Tama, S. J. Moon, and S. Lee, "Steel Surface Defect Diagnostics Using Deep Convolutional Neural Network and Class Activation Map," *Appl. Sci.*, vol. 9, no. 24, p. 5449, Dec. 2019, doi: 10.3390/app9245449.
- [36] A. Statnikov, L. Wang, and C. F. Aliferis, "A comprehensive comparison of random forests and support vector machines for microarray-based cancer classification," *BMC Bioinformatics*, vol. 9, no. 1, p. 319, 2008, doi: 10.1186/1471-2105-9-319.
- [37] S. A. Cushman, E. A. Macdonald, E. L. Landguth, Y. Malhi, and D. W. Macdonald, "Multiple-scale prediction of forest loss risk across Borneo," *Landsc. Ecol.*, vol. 32, no. 8, pp. 1581–1598, Aug. 2017, doi: 10.1007/s10980-017-0520-0.

- [38] D. Schulz, H. Yin, B. Tischbein, S. Verleysdonk, R. Adamou, and N. Kumar, "Land use mapping using Sentinel-1 and Sentinel-2 time series in a heterogeneous landscape in Niger, Sahel," *ISPRS J. Photogramm. Remote Sens.*, vol. 178, pp. 97–111, Aug. 2021, doi: 10.1016/j.isprsjprs.2021.06.005.
- [39] A. Lapini, S. Pettinato, E. Santi, S. Paloscia, G. Fontanelli, and A. Garzelli, "Comparison of Machine Learning Methods Applied to SAR Images for Forest Classification in Mediterranean Areas," *Remote Sens.*, vol. 12, no. 3, p. 369, Jan. 2020, doi: 10.3390/rs12030369.
- [40] J. S. Dramsch, "70 years of machine learning in geoscience in review," 2020, pp. 1–55.
- [41] C. Li, Z. Yu, and J. Chen, "Overview of Techniques for Improving High-resolution Spaceborne SAR Imaging and Image Quality," *J. Radars*, vol. 8, no. 6, doi: <https://doi.org/10.12000/JR19085>.
- [42] D. Amitrano *et al.*, "Sentinel-1 for Monitoring Reservoirs: A Performance Analysis," *Remote Sens.*, vol. 6, no. 11, pp. 10676–10693, Nov. 2014, doi: 10.3390/rs61110676.
- [43] F. Filippini, "Sentinel-1 GRD Preprocessing Workflow," *Proceedings*, vol. 18, no. 1, p. 11, 2019, doi: 10.3390/ecrs-3-06201.
- [44] R. Cresson, *Deep Learning for Remote Sensing Images with Open Source Software*, 1st Editio. Boca Raton: CRC Press, 2020.
- [45] Y. Guo, Y. Liu, T. Georgiou, and M. S. Lew, "A review of semantic segmentation using deep neural networks," *Int. J. Multimed. Inf. Retr.*, vol. 7, no. 2, pp. 87–93, Jun. 2018, doi: 10.1007/s13735-017-0141-z.
- [46] X. Yuan, J. Shi, and L. Gu, "A review of deep learning methods for semantic segmentation of remote sensing imagery," *Expert Syst. Appl.*, vol. 169, p. 114417, May 2021, doi: 10.1016/j.eswa.2020.114417.
- [47] D. Marmanis, K. Schindler, J. D. Wegner, S. Galliani, M. Datcu, and U. Stilla, "Classification with an edge: Improving semantic image segmentation with boundary detection," *ISPRS J. Photogramm. Remote Sens.*, vol. 135, pp. 158–172, Jan. 2018, doi: 10.1016/j.isprsjprs.2017.11.009.
- [48] R. Garg, A. Kumar, N. Bansal, M. Prateek, and S. Kumar, "Semantic segmentation of PolSAR image data using advanced deep learning model," *Sci. Rep.*, vol. 11, no. 1, p. 15365, Dec. 2021, doi: 10.1038/s41598-021-94422-y.
- [49] A. Samat, P. Gamba, P. Du, and J. Luo, "Active extreme learning machines for quad-polarimetric SAR imagery classification," *Int. J. Appl. EARTH Obs. Geoinf.*, vol. 35, no. B, pp. 305–319, Mar. 2015, doi: 10.1016/j.jag.2014.09.019.
- [50] A. Mehra, N. Jain, and H. S. Srivastava, "A novel approach to use semantic segmentation based deep learning networks to classify multi-temporal SAR data," *Geocarto Int.*, pp. 1–16, Feb. 2020, doi: 10.1080/10106049.2019.1704072.
- [51] K. Shimizu, T. Ota, and N. Mizoue, "Detecting Forest Changes Using Dense Landsat 8 and Sentinel-1 Time Series Data in Tropical Seasonal Forests," *Remote Sens.*, vol. 11, no. 16, Aug. 2019, doi: 10.3390/rs11161899.
- [52] J. Doblaz, Y. Shimabukuro, S. Sant'Anna, A. Carneiro, L. Aragão, and C. Almeida, "Optimizing Near Real-Time Detection of Deforestation on Tropical Rainforests Using Sentinel-1 Data," *Remote Sens.*, vol. 12, no. 23, p. 3922, Nov. 2020, doi: 10.3390/rs12233922.
- [53] J. A. Navarro, "First Experiences with Google Earth Engine," in *Proceedings of the 3rd International Conference on Geographical Information Systems Theory, Applications and Management*, 2017, pp. 250–255, doi: 10.5220/0006352702500255.
- [54] N. Gorelick, M. Hancher, M. Dixon, S. Ilyushchenko, D. Thau, and R. Moore, "Google Earth Engine: Planetary-scale geospatial analysis for everyone," *Remote Sens. Environ.*, vol. 202, pp. 18–27, Dec. 2017, doi: 10.1016/j.rse.2017.06.031.
- [55] F. Mohammadimanesh, B. Salehi, M. Mandianpari, E. Gill, and M. Molinier, "A new fully convolutional neural network for semantic segmentation of polarimetric SAR imagery in complex land cover ecosystem," *ISPRS J. Photogramm. Remote Sens.*, vol. 151, pp. 223–236, May 2019, doi: 10.1016/j.isprsjprs.2019.03.015.

- [56] M. Hirschmugl, J. Deutscher, C. Sobe, A. Bouvet, S. Mermoz, and M. Schardt, "Use of SAR and Optical Time Series for Tropical Forest Disturbance Mapping," *Remote Sens.*, vol. 12, no. 4, p. 727, Feb. 2020, doi: 10.3390/rs12040727.
- [57] S.-H. Lee, K.-J. Han, K. Lee, K.-J. Lee, K.-Y. Oh, and M.-J. Lee, "Classification of Landscape Affected by Deforestation Using High-Resolution Remote Sensing Data and Deep-Learning Techniques," *Remote Sens.*, vol. 12, no. 20, p. 3372, Oct. 2020, doi: 10.3390/rs12203372.
- [58] O. Ronneberger, P. Fischer, and T. Brox, "U-Net: Convolutional Networks for Biomedical Image Segmentation," May 2015, [Online]. Available: <http://arxiv.org/abs/1505.04597>.
- [59] Y. Hou, Z. Liu, T. Zhang, and Y. Li, "C-UNet: Complement UNet for Remote Sensing Road Extraction," *Sensors*, vol. 21, no. 6, p. 2153, Mar. 2021, doi: 10.3390/s21062153.
- [60] F. H. Wagner *et al.*, "Using the U-net convolutional network to map forest types and disturbance in the Atlantic rainforest with very high resolution images," *Remote Sens. Ecol. Conserv.*, vol. 5, no. 4, pp. 360–375, Dec. 2019, doi: 10.1002/rse2.111.
- [61] Z. Zhang, Q. Liu, and Y. Wang, "Road Extraction by Deep Residual U-Net," *IEEE Geosci. Remote Sens. Lett.*, vol. 15, no. 5, pp. 749–753, May 2018, doi: 10.1109/LGRS.2018.2802944.
- [62] R. Cresson, "A framework for remote sensing images processing using deep learning techniques," *IEEE Geosci. Remote Sens. Lett.*, vol. 16, no. 1, pp. 25–29, Jan. 2019, doi: 10.1109/LGRS.2018.2867949.
- [63] L. Sun, J. Chen, S. Guo, X. Deng, and Y. Han, "Integration of time series sentinel-1 and sentinel-2 imagery for crop type mapping over oasis agricultural areas," *Remote Sens.*, vol. 12, no. 1, 2020, doi: 10.3390/RS12010158.
- [64] S. Quegan, T. Le Toan, J. J. Yu, F. Ribbes, and N. Floury, "Multitemporal ERS SAR analysis applied to forest mapping," *IEEE Trans. Geosci. Remote Sens.*, vol. 38, no. 2, pp. 741–753, Mar. 2000, doi: 10.1109/36.842003.
- [65] O. Mora, P. Ordoqui, R. Iglesias, and P. Blanco, "Earthquake Rapid Mapping Using Ascending and Descending Sentinel-1 TOPSAR Interferograms," *Procedia Comput. Sci.*, vol. 100, pp. 1135–1140, 2016, doi: 10.1016/j.procs.2016.09.266.
- [66] "A Review of Interferometric Synthetic Aperture RADAR (InSAR) Multi-Track Approaches for the Retrieval of Earth's Surface Displacements," *Appl. Sci.*, vol. 7, no. 12, p. 1264, Dec. 2017, doi: 10.3390/app7121264.
- [67] R. Deo, C. Rossi, M. Eineder, T. Fritz, and Y. S. Rao, "Framework for Fusion of Ascending and Descending Pass TanDEM-X Raw DEMs," *IEEE J. Sel. Top. Appl. Earth Obs. Remote Sens.*, vol. 8, no. 7, pp. 3347–3355, Jul. 2015, doi: 10.1109/JSTARS.2015.2431433.
- [68] Bernama, "Siasat pembalakan di Hutan Simpan Kekal Yong: PEKA," *Utusan Borneo Online*, Nov. 02, 2017. <https://www.utusanborneo.com.my/2017/02/11/siasat-pembalakan-di-hutan-simpan-kekal-yong-peka> (accessed Jan. 27, 2020).
- [69] Alaska Satellite Facility, "Information and images on deforestation," 2021. <https://search.asf.alaska.edu> (accessed 10th July, 2021).
- [70] D. O. Nitti, R. F. Hanssen, A. Refice, F. Bovenga, and R. Nutricato, "Impact of DEM-Assisted Coregistration on High-Resolution SAR Interferometry," *IEEE Trans. Geosci. Remote Sens.*, vol. 49, no. 3, pp. 1127–1143, Mar. 2011, doi: 10.1109/TGRS.2010.2074204.
- [71] ESA, "Copernicus DEM - Global and European Digital Elevation Model (COP-DEM)," *ESA - European Space Agency*, 2019. <https://spacedata.copernicus.eu/web/cscda/dataset-details?articleId=394198> (accessed 18th August, 2021).
- [72] J. Ansari, S. M. Ghosh, M. Dev Behera, and S. Kumar Gupta, "A Study on Speckle Removal Techniques for Sentinel-1A SAR Data Over Sundarbans, Mangrove Forest, India," in *2020 IEEE India Geoscience and Remote Sensing Symposium (InGARSS)*, Dec. 2020, pp. 90–93, doi: 10.1109/InGARSS48198.2020.9358929.
- [73] S. Plank, "Rapid Damage Assessment by Means of Multi-Temporal SAR — A Comprehensive Review and Outlook to Sentinel-1," *Remote Sens.*, vol. 6, no. 6, pp. 4870–4906, May 2014, doi: 10.3390/rs6064870.

- [74] S. Zhang, Z. Ma, G. Zhang, T. Lei, R. Zhang, and Y. Cui, "Semantic Image Segmentation with Deep Convolutional Neural Networks and Quick Shift," *Symmetry (Basel)*, vol. 12, no. 3, p. 427, Mar. 2020, doi: 10.3390/sym12030427.
- [75] W. Yao, D. Marmanis, and M. Datcu, "Semantic segmentation using deep neural networks for SAR and optical image pairs," 2017.
- [76] L. Breiman, "Random Forests," *Mach. Learn.*, vol. 45, no. 1, pp. 5–32, Oct. 2001, doi: 10.1023/A:1010933404324.
- [77] T. Kavzoglu, "Chapter 33 - Object-Oriented Random Forest for High Resolution Land Cover Mapping Using Quickbird-2 Imagery," in *Handbook of Neural Computation*, P. Samui, S. Sekhar, and V. E. Balas, Eds. Academic Press, 2017, pp. 607–619.
- [78] M. G. Hethcoat, D. P. Edwards, J. M. B. Carreiras, R. G. Bryant, F. M. França, and S. Quegan, "A machine learning approach to map tropical selective logging," *Remote Sens. Environ.*, vol. 221, pp. 569–582, Feb. 2019, doi: 10.1016/j.rse.2018.11.044.
- [79] N. H. Agjee, O. Mutanga, K. Peerbhay, and R. Ismail, "The Impact of Simulated Spectral Noise on Random Forest and Oblique Random Forest Classification Performance," *J. Spectrosc.*, vol. 2018, p. 8316918, 2018, doi: 10.1155/2018/8316918.
- [80] S. Boonprong, C. Cao, W. Chen, X. Ni, M. Xu, and B. Acharya, "The Classification of Noise-Afflicted Remotely Sensed Data Using Three Machine-Learning Techniques: Effect of Different Levels and Types of Noise on Accuracy," *ISPRS Int. J. Geo-Information*, vol. 7, no. 7, p. 274, Jul. 2018, doi: 10.3390/ijgi7070274.
- [81] N. S. N. Shaharum, H. Z. M. Shafri, W. A. W. A. K. Ghani, S. Samsatli, M. M. A. Al-Habshi, and B. Yusuf, "Oil palm mapping over Peninsular Malaysia using Google Earth Engine and machine learning algorithms," *Remote Sens. Appl. Soc. Environ.*, vol. 17, p. 100287, Jan. 2020, doi: 10.1016/j.rsase.2020.100287.
- [82] E. Dalsasso, L. Denis, and F. Tupin, "SAR2SAR: a self-supervised despeckling algorithm for SAR images," pp. 1–7, Jun. 2020, [Online]. Available: <http://arxiv.org/abs/2006.15037>.
- [83] L. Hoyer, D. Dai, Y. Chen, A. Köring, S. Saha, and L. Van Gool, "Three Ways to Improve Semantic Segmentation with Self-Supervised Depth Estimation," Dec. 2020, [Online]. Available: <http://arxiv.org/abs/2012.10782>.